

Calcium oxalate crystal macropattern and its usefulness in the taxonomy of *Baccharis* (Asteraceae)

Paola Raeski¹, Gustavo Heiden², Andressa Novatski¹, Vijayasankar Raman³, Ikhlas Ahmed Khan³, and Jane Manfron¹

¹Universidade Estadual de Ponta Grossa

²EMBRAPA Centro de Pesquisas Agropecuarias do Clima Temperado

³University of Mississippi School of Pharmacy

January 28, 2023

Abstract

This study provides a comprehensive account of the various types of calcium oxalate crystals found in the genus *Baccharis* and assesses the exceptional value of crystal macropatterns for the taxonomy of the genus. The morphotype, occurrence and chemical composition of the crystals found in the stems and leaves are studied. The 44 species included in this study were selected based on a broad phylogeny-based sampling covering seven subgenera and 31 sections. These species were chosen to represent all the main phylogenetic lineages of *Baccharis*; thus, the sampling also represents a comprehensive coverage concerning evolutionary significance for such a large and environmentally and economically important plant group. The samples were analyzed by light microscopy, scanning electron microscopy (SEM), and energy-dispersive X-ray spectroscopy (EDS). Several morphotypes of crystals, including druses, crystal sand, styloids and prisms, were present. Based on their chemical composition, the crystals were classified as pure calcium oxalate, mixtures of oxalates and sulfates, and mixtures of oxalates, sulfates and silica. The crystal macropatterns observed in this study aid in the species identification and provide novel data for the taxonomy of *Baccharis*.

Calcium oxalate crystal macropattern and its usefulness in the taxonomy of *Baccharis* (Asteraceae)

Running title: Calcium oxalate crystals in *Baccharis* species

Authors

Paola Aparecida Raeski^{1,2*}, Gustavo Heiden³, Andressa Novatski¹, Vijayasankar Raman⁴, Ikhlas Ahmed Khan⁴, Jane Manfron^{1,2,4}

Affiliations

¹ Health Science Graduate Program, State University of Ponta Grossa, Av. Carlos Cavalcanti, 4748, Ponta Grossa, PR 84030-900, Paraná, Brazil;

² Pharmaceutical Sciences Graduate Program, State University of Ponta Grossa, Av. Carlos Cavalcanti, 4748, Paraná, Brazil.

³ Embrapa Clima Temperado, Pelotas, Rio Grande do Sul, Brazil.

⁴ National Center for Natural Products Research, School of Pharmacy, The University of Mississippi, Mississippi, MS 38677, USA.

***Corresponding author:** Paola A. Raeski (Email: paola.ap.raeski@gmail.com)

Abstract

This study provides a comprehensive account of the various types of calcium oxalate crystals found in the genus *Baccharis* and assesses the exceptional value of crystal macropatterns for the taxonomy of the genus. The morphotype, occurrence and chemical composition of the crystals found in the stems and leaves are studied. The 44 species included in this study were selected based on a broad phylogeny-based sampling covering seven subgenera and 31 sections. These species were chosen to represent all the main phylogenetic lineages of *Baccharis*; thus, the sampling also represents a comprehensive coverage concerning evolutionary significance for such a large and environmentally and economically important plant group. The samples were analyzed by light microscopy, scanning electron microscopy (SEM), and energy-dispersive X-ray spectroscopy (EDS). Several morphotypes of crystals, including druses, crystal sand, styloids and prisms, were present. Based on their chemical composition, the crystals were classified as pure calcium oxalate, mixtures of oxalates and sulfates, and mixtures of oxalates, sulfates and silica. The crystal macropatterns observed in this study aid in the species identification and provide novel data for the taxonomy of *Baccharis*.

Keywords : crystal shapes, energy-dispersive X-ray spectroscopy, light microscopy, polarized light microscopy, scanning electron microscopy

Research Highlights

Most species of *Baccharis* have a specific crystalline pattern. Each species produces a crystal morphotype or a set of morphotypes specific to it. The crystals observed are formed by calcium oxalate.

Introduction

Crystals of calcium oxalate are common in Angiosperms and occur in most tissues and organs in the plant. They are formed from endogenously synthesized oxalic acid and calcium taken from the environment, shaped and accumulated in species-specific morphologies (Meric, 2009). The morphotypes of crystals and their locations (crystal macropatterns) are determined by gene expression and are often species-specific (Horner et al., 2012). Therefore, these features are applicable in plant systematics, ecophysiological and phylogenetic studies (Lersten & Horner, 2011; Silva et al., 2014).

The most common minerals formed by plants are calcium oxalate, calcium carbonate and silica (Bouropoulos et al., 2001). The excess of calcium is usually precipitated in calcium salts such as carbonate, citrate, malate, oxalate, phosphate and silicate (Weiner & Dove, 2003). Calcium sulfate crystals are rare in plants (He et al., 2012).

The functions of crystals in plants vary depending on their location and morphotype. They act as an internal reservoir for calcium, provide tissue rigidity, osmotic regulation, ionic balance, remove calcium, magnesium, oxalic acid, aluminum and other heavy metals, act as a protective device against herbivory, and regulate uptake and reflection of solar energy (Pritchard et al., 2000; Franceschi & Nakata, 2005; He et al., 2012).

In Asteraceae, particularly in *Baccharis* L., the crystals are generically described as incidental observations and in situ analyzes of the chemical composition of crystals are scarce or absent (Budel et al., 2003; Budel et al., 2004; Souza et al., 2011; Santos et al., 2012). The genus comprises 442 species (Heiden & Bonifacino, 2021), is monophyletic (Heiden et al., 2019), and presents similarities in the morphological features among several groups of closely related species causing challenges in taxonomic studies of the group (Bobek et al., 2016; Budel et al., 2018; Almeida et al., 2021).

Considering that the morphology and occurrence of crystals within plants are genetically controlled and are specific to a particular species, the present study aimed to describe the macropatterns and chemical compositions of crystals in *Baccharis* species. Forty-four species representing all the seven subgenera, 31 of the 47 sections, and 44 of the 442 species are analyzed. They represent 100% subgenera, 66% of the sections and 10% of the species diversity within the genus. The comprehensive evolutionary sampling covers all the main lineages currently recognized based on phylogenetic grounds allowing to evaluate their utility in taxonomy and interspecific differentiation.

Material and Methods

Plant material

Species prioritization was designed to sample at least one species from the 31 main clades and all subgenera sampled and retrieved in the phylogenetic analyses of *Baccharis* (Heiden et al., 2019) and at the same time represents 10% of the species richness of the genus. Tissue samples of the 44 chosen *Baccharis* species were obtained from herbarium specimens deposited at the ECT herbarium of Embrapa Clima Temperado, Pelotas in Rio Grande do Sul, Brazil. The place and date of collection of these specimens, their voucher numbers and analyzed organs are summarized in Table 1. Access to the botanical material was approved and licensed by CGEN/SISGEN and registered under code AFEEC2B.

Table 1. *Baccharis* (Asteraceae) sampling species list, subgenus and section placement, collection location details, voucher information and analyzed organs studied to investigate calcium oxalate crystals macropatterns.

Tissue clearings

Herbarium sample fragments were collected from each specimen, hydrated in deionized water at 60 °C overnight, treated with commercial household bleach (5.25% sodium hypochlorite) until translucent, and carefully washed in running tap water.

Polarized light microscopy (PM)

The cleared and mounted specimens were sectioned, mounted on glass slides in a drop of 50% glycerin and analyzed using a Nikon Eclipse E600POL polarizing microscope equipped with Nikon DSFiv camera systems and Nikon Elements imaging software (Nikon Inc., Tokyo, Japan).

Scanning Electron Microscopy (SEM)

The samples were fixed in FAA 70 (formalin-acetic acid-alcohol) for 3 days and washed in distilled water. Then, the samples were dehydrated in a series of ethanol solutions (70, 80, 90 and 100%) and dried in a Balzers CPD 030 critical point dryer (BAL-TEC AG, Balzers, Liechtenstein) supplied with liquid CO₂ and then coated with gold using a Quorum (model SC7620) sputter coater. Photomicrographs were prepared using a Mira 3 Field-Emission SEM (Tescan, Brno-Kohoutovice, Czech Republic).

Energy Dispersive X-ray spectroscopy (EDS)

During the SEM procedure, EDS analysis was performed to obtain the chemical composition of the crystals. This analysis was randomly made for the crystals, and the cells devoid of crystals as a control, using an EDS detector (Oxford Instruments, Oxford, UK) attached to the SEM. Aztec software (Oxford Instruments, Oxford, UK) was used to perform the EDS analysis. SEM and EDS were performed at the Multiuser Laboratory Complex (C-Labmu) at the State University of Ponta Grossa, Paraná, Brazil.

Raman Spectroscopy (RS)

The crystals were measured using a Horiba LabRAM HR Evolution spectrophotometer with an excitation laser (785 nm) and a grid of 300 lines/mm. Synapse detector and a microscope coupled with a 50X objective lens, with numerical aperture 0.4. Thirty averages were taken for each measurement, with an exposure time of 15 seconds, in the range of 100 to 1600 cm⁻¹.

Crystal shapes and locations

Crystal forms were compared with published images (Franceschi & Horner, 1980; Franceschi & Nakata, 2005; Chvátal, 2007; He et al., 2012; Raman et al., 2014; Silva et al., 2014; Smith, 2012; Sun et al., 2015; Uloth et al., 2015; Brito et al., 2021). The location of the crystal forms was determined by visually identifying a specific tissue by focusing through the cleared material.

Results and Discussion

Morphology and distribution of crystals

The crystals in all cleared tissues were easily detected since the clearing technique rendered the tissues translucent. Morphology and occurrence of crystals in various tissues of the analyzed species were observed using PM and SEM, and the results are shown in Table 2.

A total of 44 *Baccharis* species, representing about 10% of the genus, were analyzed using PM, SEM, EDS and RS to determine if the crystals were present in the species, evidence the crystalline morphotypes and analyze their chemical composition.

The shapes and sizes of the crystals varied considerably among the species (Fig 1, 2, 3 and 4). Only *B. oblongifolia* and *B. tarchonanthoides* did not have crystals in the leaves and stems. Other species displayed one or more types of crystals, such as arrow-shaped (Fig.1A-D and 1O), bipyramidal (Fig.1E-K and 1P-V), cuneiform (Fig. 1L-N and 1W-Y), crystal sand (Fig.2A-S), druse (Fig. 3A-K), dodecahedron (Fig. 4A), pyramidal (Fig.4B-C and 4L-M), styloid (Fig.4D-G and 4N-U), tabular (Fig.4I-K), and trigonal prism (Fig. 4H).

In the present study, crystals were found in the leaves and stems. Crystals have been reported in the perimedullary region of stems in several *Baccharis* species (Budel & Duarte, 2008; Souza et al., 2011; Oliveira et al., 2011; Jasinski et al., 2014; Barreto et al., 2015; Bobek et al., 2015; Almeida et al., 2021)."

Table 2: Morphotype and localization of crystals in the 44 investigated *Baccharis* (Asteraceae) species.

[ar - arrow-shaped crystal; bps - bipyramidal simple; bpq – bipyramidal square; bpr – rectangular bipyramidal; cn – cuneiform crystal; dr – druse crystal; do – dodecahedron crystal; rp - rectangular pyramid; sp - square pyramids; st – styloid; rb – rhomboid crystal; tp – triangular prism crystal; sar – sand arrow-shaped; sbo – sand bow tie-shaped; sbp – sand bipyramidal; scn – sand cuneiform; sro – sand rounded; srp – sand rectangular parallelepiped; ssp – sand square parallelepiped; sst – sand styloid; srb – sand rhomboid; arb - aggregate crystals rhomboid; ft - flagelliform trichome; gt - glandular trichomes; ngt - non-glandular trichome].

Arrow-shaped crystals (ar) (Fig. 1A-D, O) are found in the stems of *B. aliena* , *B. aphylla* , *B. articulata* , *B. curitybensis* , *B. dracunculifolia* , *B. dubia* , *B. genistelloides* , *B. gnaphalioides* , *B. helicrysoides* , *B. illinita* , *B. linearifolia* , *B. macrophylla* , *B. nitida* , *B. patens* , *B. platypoda* , *B. polifolia* , *B. potrerillana* , *B. racemosa* , *B. ulicina* , and *B. uncinella* . They are also found in the foliar epidermis of *B. dubia* , *B. paniculata* and *B. ulicina*. This type of crystal has a pointed end and the other end with a V-shaped recess, resembling an arrowhead.

Three shapes of bipyramidal crystals were found: simple (bps), squared (bpq) and rectangular (bpr). The simple bipyramidal crystals are characterized by the direct union of two pyramids (Fig. 1F-G and 1S-T) and was observed in the stems of *B. aliena* , *B. articulata* , *B. conyzoides* , *B. coridifolia* , *B. curitybensis* , *B. dracunculifolia* , *B. helicrysoides* , *B. illinita* , *B. microdonta* , *B. pauciflosculosa* , *B. punctulata* , *B. racemosa* , *B. uncinella* and *B. wagenitzii* . It also occurs in the leaf epidermis of *B. megapotamica* , yet more sparsely. It was also found in the perimedullary region of *B. dracunculifolia* in the study by Budel et al. (2004).

The bpq crystals contains a thin base between the union of the two pyramids (Fig. 1E, I-J, Q), observed in the perimedullary region of stem of *B. curitybensis* , *B. dracunculifolia* , *B. helicrysoides* , *B. illinita* , *B. nitida* , *B. paniculata* , *B. platypoda* , *B. pluricapitulata* , *B. reticularioides* , *B. salicifolia* , *B. sphenophylla* , *B. tridentata* , *B. ulicina* and *B. uncinella* . In addition, this morphotype was found in the leaf epidermis of *B. curitybensis* and mesophyll of *B. nitida* . This type of crystal is commonly found in the genus, such as in *B. trilobata* A.S.Oliveira & Marchiori and was named square bipyramids by Bobek et al. (2016).

The rectangular bipyramidal (bpr) has a thick base between the union of the two pyramids (Fig. 1H; 1K; 1P and 1U-V), this type was observed in the perimedullary region of stem of *B. articulata* , *B. curitybensis* , *B. dracunculifolia* , *B. megapotamica* , *B. nitida* , *B. tridentata* , *B. reticularioides* and *B. ulicina* . Also, *B.*

megapotamica showed bpr type in the leaf epidermis. This type is frequently found in *Baccharis* (Budel et al., 2015) and was named as elongated square bipyramids by Bobek et al. (2016).

Cuneiform crystals (Fig. 1L-N and 1W-Y) were observed in 28 of the 44 studied species of *Baccharis*. They occur in the perimedullary region of stems of *B. aliena*, *B. aphylla*, *B. articulata*, *B. caespitosa*, *B. ciliata*, *B. curitybensis*, *B. dracunculifolia*, *B. dubia*, *B. genistelloides*, *B. glomeruliflora*, *B. gnaphalioides*, *B. helicrysoides*, *B. illinita*, *B. linearifolia*, *B. macrophylla*, *B. platypoda*, *B. polifolia*, *B. potrerillana*, *B. punctulata*, *B. racemosa*, *B. salicifolia*, *B. sphenophylla*, *B. ulicina* and *B. umbelliformis*; in the leaf mesophyll of *B. gnaphalioides*; and in the leaf epidermis of *B. helicrysoides*, *B. megapotamica*, *B. paniculata* and *B. umbelliformis*.

Figure 1. *Baccharis* stems in cross-section [SEM (A-D); PM (O-Y)]. *B. articulata* (A;K), *B. aphylla* (B;O), *B. polifolia* (C), *B. linearifolia* (D;L), *B. curytibensis* (E), *B. dracunculifolia* (F;I), *B. uncinella* (G), *B. aliena* (H;W;Y), *B. puricapitulata* (J), *B. patens* (M-N), *B. conyzoides* (P-R;T), *B. megapotamica* (S;U), *B. nitida* (V), *B. ciliata* (X). [ar- arrow-shaped crystal; bps - bipyramidal simple; bpq - bipyramidal square; bpr - rectangular bipyramidal; cn - cuneiform crystal]. Bars: A-D,I-J = 5µm; E,G,H,K-O,S= 10 µm; P-R,U-Y = 20 µm; T = 25 µm.

Among the various types of crystals found in plants, crystal sand is relatively common. It consists of a mass of small (2-5 µm) individual crystals within a single cell, assuming different forms (Upton et al., 2011). Most studies have described these structures simply as crystal sands without detailing the micromorphology of the crystals (Konyar et al., 2014; Santos et al., 2015; Capacio & Belonias, 2018; Gribner et al., 2022). In the present study, nine morphotypes of crystal sands are recorded in the perimedullary region of stems of *Baccharis* species: arrow-shaped (sar) (Fig. 2A) in *B. pauciflosculosa*, *B. platypoda*, *B. reticularioides* and *B. thymifolia*; bipyramidal (sbp) (Fig. 2E-G) in *B. paniculata*, *B. potrerillana*, and *B. pluricapitulata*; cuneiform (scn) (Fig. 2H) in *B. thymifolia*; rounded (sro) (2I-J) in *B. articulata*, *B. nitida*, *B. platypoda* and *B. sphenophylla*; rectangular parallelepiped (srp) (Fig. 2K) in *B. nitida* and *B. reticularioides*; square parallelepiped (ssp) (Fig. 2L-M) in *B. megapotamica*, *B. pauciflosculosa* and *B. reticularioides*; styloid (sst) (Fig. 2N-O) in *B. aliena*, *B. articulata*, *B. dracunculifolia*, *B. helicrysoides*, *B. illinita*, *B. nitida*, *B. pluricapitulata*, *B. potrerillana*, *B. racemosa*, *B. salicifolia*, *B. umbelliformis* and *B. wagenitzii*; rhomboid (srb) (Fig. 2P-R) in *B. macrophylla*, *B. platypoda*, *B. pluricapitulata*, *B. thymifolia* and *B. uncinella*; and bow tie-shaped (sbo) (Fig. 2B-D) in *B. articulata*, *B. dubia* and *B. platypoda*. Bow tie-shaped crystal sand is found and named in the present work for the first time.

Figure 2 – Crystal sand in *Baccharis* stems in cross-section. [SEM (A-S)]. *B. uncinella* (A); *B. articulata* (B-C;I); *B. platypoda* (D;J;S); *B. pluricapitulata* (E); *B. paniculata* (F); *B. potrerillana* (G); *B. nitida* (H;O); *B. reticularioides* (K); *B. pauciflosculosa* (L); *B. megapotamica* (M); *B. helicrysoides* (N); *B. thymifolia* (P-Q); *B. macrophylla* (R). [sar - sand arrow-shaped; sbo - sand bow tie-shaped; sbp - sand bipyramidal; scn - sand cuneiform; sro - sand rounded; srp - sand rectangular parallelepiped; ssp - sand square parallelepiped; sst - sand styloid; srb - sand rhomboid; arb - aggregate crystals rhomboid]. Scale bar: B-C;F;H = 2µm; A;D-E;G;I;K-S = 5 µm; J = 10 µm.

Another crystalline type identified in the present study was druse (Fig. 3A-K), characterized by a cluster of diamond-shaped crystals with sharp points. This type is observed in the perimedullary region of stems (Fig. 3A and 3D) in *B. potrerillana*, *B. racemosa*, *B. trinervis* and *B. wagenitzii*; and in the foliar epidermis of *B. arguta*, *B. articulata*, *B. curitybensis*, *B. paniculata*, *B. patens*, *B. trinervis* and *B. wagenitzii*. In *B. ulicina*, druses are also found in the foliar epidermis (Fig. 3G-K) and mesophyll. In relation to the biserial glandular trichomes, only druses were found in the apical cells (Fig. 3B-C; 3E-F) of *B. aliena*, *B. arguta*, *B. articulata*, *B. boliviensis*, *B. caespitosa*, *B. ciliata*, *B. curitybensis*, *B. dracunculifolia*, *B. glomeruliflora*, *B. gnaphalioides*, *B. linearifolia*, *B. macrophylla*, *B. microdonta*, *B. potrerillana*, *B. nitida*, *B. platypoda*, *B. pluricapitulata*, *B. polifolia*, *B. sphenophylla*, *B. tridentata*, *B. umbelliformis* and *B. uncinella*. In the present work, only *B. arguta* shows druses in the 7-8-celled, uniseriate, conical non-glandular trichomes (Fig. 3H-I), which can be considered an anatomical marker for the species.

Figure 3 – Calcium oxalate druses in *Baccharis* species. (A,D – Stem; B-F – glandular trichome; H,I – non-glandular trichome; G-K – foliar epidermis). [SEM (A); PM (B-K)]. *B. wagenitzii* (A,D); *B. aliena* (B); *B. sphenophylla* (C); *B. microdonta* (E-F); *B. arguta* (G-J); *B. tridentata* (K). [dr – druse crystal]. Scale bar: A,D = 10µm; B,C,E,F = 20 µm; G-K = 50 µm.

The presence and the type of trichomes are significant anatomical markers for *Baccharis* species. The presence of druses in trichomes is an additional characteristic helpful in species identification. The presence of druses in the apical cells of biseriate glandular trichomes in *Baccharis* was first reported by Budel et al. (2018) for *B. microdonta* and *B. sphenophylla*, as also found in the present study.

Baccharis aliena and *B. umbelliformis* present a peculiar type of crystal in the perimedullary region of stem. The crystal is formed by 12 pentagonal regular faces (Fig 4A), it was named dodecahedron by Smith (2012). To the best of our knowledge, this type of crystal has not previously been reported in *Baccharis* species.

Two types of pyramid-shaped prismatic crystals, rectangular pyramids (rp) and square pyramids (sp), were observed. The base of the pyramid is rectangular in rp (Fig. 4B-C), whereas is square in sp (Fig. 4L-M). The rp crystals appeared in the perimedullary region of stem of *B. articulata*, *B. racemosa*, *B. ulicina* and *B. uncinella*. The sp crystal appeared only in the leaf epidermis of *B. dubia*. Type rp has not been mentioned yet in the literature, whereas sp was found in *Baccharis* species, such as *B. crispa* Spreng., *B. microcephala* DC. (Budel & Duarte, 2009) and *B. glaziovii* Baker (Jasinski, 2016).

The most common type of crystals found in the analyzed species are styloids (st) (Fig. 4D-G and 4N-U). Styloids were frequently observed in *Baccharis* species (Jasinski et al., 2014; Budel et al., 2015, Bobek et al., 2016, Jasinski, 2016). Thirty eight of the 44 species studied have styloid crystals (Table 2). They are long, prism-like with plane faces, occurring singly or in pairs. They have pointed ends in frontal view or are truncated in the lateral face (Franceschi & Horner, 1980; Raman et al., 2014). Styloids were found in the rhizome of *B. acaulis*, in the perimedullary region of stem of *B. aliena*, *B. aphylla*, *B. arguta*, *B. articulata*, *B. boliviensis*, *B. caespitosa*, *B. ciliata*, *B. coridifolia*, *B. curitybensis*, *B. dracunculifolia*, *B. dubia*, *B. genistelloides*, *B. glomeruliflora*, *B. gnaphalioides*, *B. helicrysoides*, *B. illinita*, *B. linearifolia*, *B. macrophylla*, *B. megapotamica*, *B. microdonta*, *B. nitida*, *B. paniculata*, *B. patens*, *B. pluricapitulata*, *B. polifolia*, *B. potrerillana*, *B. punctulata*, *B. racemosa*, *B. salicifolia*, *B. sphenophylla*, *B. thymifolia*, *B. tridentata*, *B. trinervis*, *B. ulicina*, *B. umbelliformis*, *B. uncinella* and *B. wagenitzii*, in the mesophyll of *B. aliena*, *B. glomeruliflora*, *B. gnaphalioides* and *B. salicifolia* and in the foliar epidermis of *B. arguta*, *B. boliviensis*, *B. coridifolia*, *B. dracunculifolia*, *B. dubia*, *B. genistelloides*, *B. helicrysoides*, *B. linearifolia*, *B. megapotamica*, *B. paniculata*, *B. pluricapitulata*, *B. polifolia*, *B. potrerillana*, *B. racemosa*, *B. tridentata*, *B. ulicina*, *B. umbelliformis*, *B. uncinella* and *B. wagenitzii*.

Rhomboid or diamond-shaped crystals (Fig. 4I-K) are found in the perimedullary region of stems of *B. aphylla*, *B. articulata*, *B. ciliata*, *B. genistelloides*, *B. linearifolia*, *B. patens*, *B. platypoda*, *B. polifolia*, *B. potrerillana*, *B. ulicina* and *B. umbelliformis*. In *B. platypoda*, these crystals are grouped to form aggregate crystals (Figure 2S). This type of crystals has also been reported in *B. trilobata* (Bobek et al., 2016).

In the perimedullary region of stems of *B. aliena*, *B. ciliata* and *B. illinita*, a triangular prism crystal (tp) is seen. It is characterized as a regular prism with the ends made up of triangles (Fig. 4H). This type of crystal has not been reported for the genus *Baccharis* before.

Figure 4. *Baccharis* spp. (A-C; E-O;S;U – stem; D;P;T – mesophyll; Q-R – foliar epidermis). [SEM (A-K); MP (L-U)]. *B. aliena* (A); *B. ulicina* (B-C); *B. illinita* (D; H); *B. helicrysoides* (E;O;R;U); *B. glomeruliflora* (F;P-Q); *B. articulata* (G); *B. genistelloides* (I); *B. linearifolia* (J); *B. potrerillana* (K); *B. dubia* (L-M); *B. gnaphalioides* (N;S); *B. wagenitzii* (T). [do – dodecahedron crystal; rp – rectangular pyramid; st – styloid; tp – triangular prism crystal; rb – rhomboid crystal; sp – square pyramids]. Scale bar: B-C;G;I-K = 5 µm; A;D-F;H;L-M = 10 µm; N-U = 20 µm.

Elemental composition of crystals

The most common chemical composition of crystals found in plant species is calcium oxalate (CaC_2O_4), appearing in more than 215 plant families. However, other compositions can also occur, such as calcium carbonate (CaCO_3) crystals, or even silica crystals (SiO_2) (Bosqueiro, 1995; Webb, 1999). Crystals in plants have been reported as calcium oxalate using EDS in many studies (Lersten & Horner, 2011; Saulle et al., 2018; Santos et al., 2018; Almeida et al., 2020; Klider et al., 2020; Brito et al., 2021; D’Almeida et al., 2021; Pauzer et al., 2021; Gribner et al., 2022). Only a few studies have reported calcium sulfate crystals (Storey & Thomson, 1994; Pritchard et al., 2000; He et al., 2012).

Qualitative X-ray microanalyses showed that the crystals observed in this study are formed by calcium oxalate. This aligns with their shapes and birefringence feature observed in polarized light (Franceschi & Horner, 1980; Raman et al., 2014). The EDS spectra showed prominent peaks for calcium, carbon, and oxygen (Fig. 5A-D). A noise peak at 0keV, and a prominent unlabeled peak near 2keV representing gold (Au) used for coating the samples, are also visible in the spectra.

Figure 5 – EDS spectra of crystals in *Baccharis* species: *B. curitybensis* (A); *B. dracunculifolia* (B); *B. ciliata* (C); *B. articulata* (D); *B. boliviensis* (E); *B. oblongifolia* (F); the samples were coated with gold (Au). [A – bipyramidal square; B – bipyramidal simple; C – cuneiform; D – rectangular pyramid; E-F – control cell].

Raman Spectroscopy

The hydration status of calcium oxalate crystals as well as the proportion of calcium and the presence of contaminating elements can influence the determination of the morphology of the crystals (Franceschi & Nakata, 2005). Hydration regulates crystal morphology by distributing and coordinating calcium and oxalate ions (Ishii, 1991). Two hydration states are frequently found, the monohydrate state known as whewellite and the dihydrate state known as weddellite. Whewellite is found in crystals considered as a monocyclic system, such as styloid, cuneiform and tabular crystals. In contrast, weddellite is present in crystals of the tetragonal system, such as pyramidal and bipyramidal crystals (Franceschi & Horner, 1980; Frey-Wyssling, 1981). Both hydration states were observed in *Baccharis* species using Raman spectroscopy. Weddellite spectra were observed mainly in bipyramidal crystals, while whewellite spectra were observed in the styloids (Fig. 6). This characteristic further reinforces the importance of hydration status in crystal morphology.

Figure 6 – Raman spectroscopy: The hydration status of calcium oxalate crystals in *Baccharis* spp. [Whewellite state (A-C); Weddellite state (D-F)].

Of the 44 species, 42 presented a set of crystal morphotypes. No crystals were observed in *B. oblongifolia* and *B. tarchonanthoides*. Two species, *B. linearifolia* and *B. polifolia*, showed similar crystalline patterns; however, the sizes of the crystals in these species are different, which can help differentiate the species.

Morphologies and locations of crystals are genetically controlled and a particular species will form only a specific crystal type or set of crystal morphologies (Franceschi & Nakata, 2005). The combination of more than one crystalline form can be present as the characteristic of the species, section, subgenus or genus, giving support to the taxonomy (Al-Rais et al., 1971). In this study, notable differences in the crystalline macropattern were observed in the sections *Aphyllae*, *Angustifoliae*, *Canescentes*, *Cylindricae*, *Oblongifoliae*, *Racemosae* and *Tachonanthoides*. In section *Aphyllae*, both *B. aphylla* and *B. articulata* presented styloid, cuneiform, tabular and arrow-like crystals in the perimedullary region of stem. In section *Angustifoliae*, the species *B. arguta* and *B. ulicina* presented styloid crystals in the perimedullary region of stem and leaf epidermis, and druses in the leaf epidermis. *B. ciliata* and *B. macrophylla* of section *Oblongifoliae* had styloid and cuneiform crystals in the perimedullary region of stem, besides both the species presenting druse in the glandular trichomes. The section *Racemosae* represented in this study by *B. dracunculifolia* and *B. uncinella* showed bipyramidal type 1, bipyramidal type 2, styloid and arrow type crystals in the perimedullary region of stem and styloids in the leaf epidermis. The crystal types in section *Aphyllae* were also found in section *Canescentes*, represented by *B. ganaphalioide*s and *B. helicyroides*, except for tabular morphotypes. *Agglomeratae* section with the species *B. pauciflosculos*a, *B. platypoda* and *B. reticularioides* had crystal sands of arrow-shaped prisms in the perimedullary region of stem. In *B. linearifolia* and *B. microdonta*

belonging to section *Cylindricae* , styloids in the perimedullary region of stems and druses in the glandular trichomes were present. In the section *Tarchonanthoides* , the species *B. curitybensis* and *B. patens* had styloids, cuneiform and arrow-shaped crystals in the perimedullary region of stem and druses in the glandular trichomes. Each species within a section presented the same crystal macropattern but with at least one morphotype that differentiated one species from another. Further studies focusing on sampling as many species as possible within subgenera or sections could provide information on the shared or unique occurrence of crystal macropatterns that could be taxonomically informative to recognize infrageneric taxa or as species-specific anatomical markers.

Conclusions

This study showed that most species of *Baccharis* belonging to distantly or closely phylogenetically related species have a specific crystalline pattern, except for *B. oblongifolia* and *B. tarchonanthoides* in which no crystals were observed. Several morphotypes of crystals, including druses, crystal sand, styloids and prisms, were found. Raphides were not observed in any of the studied species. Various shapes of prisms, such as arrow-shaped, bipyramidal, cuneiform, polyhedron, pyramidal, tabular, and trigonal prisms, were observed. Based on their chemical composition, birefringence and crystal shape, the crystal macropatterns observed in this study can aid in the species identification and taxonomy of *Baccharis* .

In the present study, it was also observed that each species produces a crystal morphotype or a set of morphotypes specific to it. Thus, the presence or absence of a particular crystal morphotype and its location within the plant are crucial anatomical markers that can be used to resolve and build better classifications and aid in solving taxonomic problems. Also, the features highlighted in the present study provide phylogenetic relationships of the taxa in the genus *Baccharis* .

Acknowledgments

We acknowledge the C-Labmu Center at the State University of Ponta Grossa (UEPG) for the SEM and EDS facilities. This study was financed (Finance Code 88881.119611/2016-01 and 88887.634811/2021) by the Coordenação de Aperfeiçoamento de Pessoal de Nível Superior of Brasil (CAPES). GH acknowledges CNPq (PQ2 314590/2020-0) for the productivity research fellowship and the LinnéSys Fund 2021.

References

- Almeida, V. P.; Raman V.; Raeski P. A.; Urban A. M.; Swiech J. N.; Miguel M. D.; Farago P. V.; Khan I. A.; Budel J. M. (2020). Anatomy, micromorphology, and histochemistry of leaves and stems of *Cantinoa althaeifolia* (Lamiaceae). *Microsc Res Techniq* **83** (5), 551-557.
- Almeida, V.P.; Heiden G.; Raman V.; Novatski A.; Bussade J. E.; Farago P. V.; Manfron J. (2021). Microscopy and Histochemistry of Leaves and Stems of *Baccharis* Subgenus *Coridifoliae* (Asteraceae) Through LM and SEM-EDS. *Microsc Microanal* **27** (5), 1273–1289.
- Al-Rais, A. H.; Myers, A.; Watson, L. (1971) The isolation and properties of oxalate crystals from plants. *Ann Bot* **35** , 1213-1218.
- Barreto, I. F.; Paula, J. P.; Farago, P. V.; Duarte, M. R.; Budel, J. M. (2015). Pharmacobotanical study of the leaves and stems of *Baccharis ochracea* Spreng. for quality control. *Lat Am J Pharm* **34** , 1497–1502.
- Bobek, V. B.; Almeida, V. P.; Pereira, C.; Heiden, G.; Duarte, M. R.; Budel, J. M.; Nakashima, T. (2015). Comparative pharmacobotanical analysis of *Baccharis caprariifolia* DC. and *B. erioclada* DC. From Campos Gerais, Paraná, Southern Brazil. *Lat Am J Pharm* **34** (7), 1396-1402.
- Bobek, V. B.; Heiden, G.; Oliveira, C. F.; Almeida, V. P.; Paula, J. P. P.; Farago, P. V.; Nakashima, T.; Budel, J. M. (2016). Comparative analytical micrographs of “vassouras” (*Baccharis* , Asteraceae). *Rev Bras Farmacogn* **26** , 665-672.
- Bosqueiro, A. L. D. (1995). Metabólitos secundários em plantas. *Revista Ciência e Educação*. **13** (2), 91-96.

- Bouropoulos, N.; Weiner, S.; Addadi, L. (2001). Calcium oxalate crystals in tomato and tobacco plants: Morphology and in vitro interactions of crystal-associated macromolecules. *Chem Eur J* 7 (9), 1881-1888.
- Brito P. S.; Sabedotti C.; Flores T.B.; Raman V.; Bussade J. E.; Farago P. V.; Manfron J. (2021). Light and scanning electron microscopy, energy dispersive x-ray spectroscopy, and histochemistry of *Eucalyptus tereticornis* . *Microsc Microanal* 27 , 1295–1303.
- Budel, J. M.; Duarte, M. R.; Santos, C. A. M. (2003). Caracteres morfo-anatômicos de *Baccharis gaudichaudiana* DC., Asteraceae. *Acta Farm Bonaerense* 22 (4), 313-320.
- Budel, J. M.; Duarte, M. R.; Santos, C. A. M. (2004). Stem morpho-anatomy of *Baccharis cylindrica* (Less.) DC. (Asteraceae). *Braz J Pharm Sci* 40 (1), 93-99.
- Budel, J. M.; Duarte, M. R. (2008). Estudo farmacobotânico de folha e caule de *Baccharis uncinella* DC. Asteraceae. *Lat Am J Pharm* 27 (5), 740-746.
- Budel, J. M.; Duarte, M. R. (2009). Análise morfoanatômica comparativa de duas espécies de carqueja: *Baccharis microcephala* DC. e *B. trimeria* (Less.) DC., Asteraceae. *Braz J Pharm Sci* 45 (1), 75-85.
- Budel, J. M.; Paula, J. P.; Santos, V. L. P.; Franco, C. R. C.; Farago, P. V.; Duarte, M. R. (2015). Pharmacobotanical study of *Baccharis pentaptera* . *Rev Bras Farmacogn* 25 , 314-319.
- Budel, J. M.; Raman, V.; Monteiro, L. M.; Almeida, V. P.; Bobek, V. B.; Heiden, G.; Takeda, I. J. M; Khan, I. A. (2018). Foliar Anatomy and microscopy of six Brazilian species of *Baccharis* . *Microsc Res Techniq* 81 (8),1-30.
- Capacio, A. F. Z.; Belonias, B. S. (2018). Occurrence and variation of calcium oxalate crystals in selected medicinal plant species. *Ann Trop Res* 40 (2), 45-60.
- Chvátal, M. (2007). *Mineralogia para principiantes: Cristalografia* [Mineralogy for beginners: Crystallography]. Sociedade Brasileira de Geologia.
- D’Almeida W.; Monteiro L. M.; Raman V.; Rehman J. U.; Paludo K. S.; Maia, B. H. L. N. S.; Casapula I.; Khan I. A.; Farago P. V.; Budel J. M. (2021). Microscopy of *Eugenia involucrata* , Chemical Composition and Biological Activities of the Volatile Oil. *Rev Bras Farmacogn* 31 , 239-243.
- Franceschi, V. R.; Horner, H. T. (1980). Calcium oxalate crystals in plants. *Bot Rev* 46 (4), 361-416.
- Franceschi, V. R.; Nakata, P. A. (2005). Calcium oxalate in plants: formation and function. *Annu Rev Plant Biol* 56 , 41–71.
- Frey-Wyssling, A. (1981). Crystallography of the two hydrates of crystalline calcium oxalate in plants. *Am J Bot* 68 (1), 130–141.
- Gribner, C.; Barbosa, V.; Monteiro, L.M.; Swiech, J.N.D.; Raman, V.; Manfron, J.; Miguel, O.G.; Montruchio, D.P.; de Fátima Gaspari Dias, J. (2022). Microscopic investigations of *Ocotea paranaensis* - A Brazilian endemic and endangered species. *Microsc Res Tech*. doi: 10.1002/jemt.24186. Epub ahead of print.
- He, H.; Bleby, T.M.; Veneklaas, E.J.; Lambers, H.; Kuo, J. (2012). Morphologies and elemental compositions of calcium crystals in phyllodes and branchlets of *Acacia robeorum* (Leguminosae: Mimosoideae). *Ann Bot* 109 (5), 887-896.
- Heiden, G.; Antonelli, A.; Pirani, A. A. J. R. (2019). A novel phylogenetic infrageneric classification of *Baccharis*(Asteraceae: Astereae), a highly diversified American genus. *Taxon* 58 (5), 1048-1081.
- Heiden, G.; Bonifacino, J. M. (2021) *Baccharis* L. (Astereae): From Nova Scotia to Cape Horn. *TICA* 1 , 12-35.
- Horner, H. T; Wanke, S.; Samain, M. S. (2012) A comparison of leaf crystal macropatterns in the two sister genera *Piper* and *Peperomia* (Piperaceae). *Am J Bot* 99 (6), 983-997.

- Ishii, Y. (1991) Three kinds of calcium oxalate hydrates. *Nippon kagaku kaishi* 63 , 63-70.
- Jasinski, V. G.; Silva, R. Z.; Pontarolo, R.; Budel, J. M.; Campos, F. R. (2014) Morpho-anatomical characteristics of *Baccharis glaziovii* in support of its pharmacobotany. *Rev Bras Farmacogn*24 , 609-616.
- Jasinski, V. C. G. (2016). Avaliação morfoanatomica, fitoquímica e biológica de *Baccharis glaziovii* Baker (Asteraceae) [Dissertation]. Universidade Federal do Paraná.
- Klider, L. M.; Machado, C. D.; Almeida, V. P.; Tirloni, C. A. S.; Marques, A. A. M.; Palozi, R. A. C.; Lorençone, B. R.; Romão, P. V. M.; Guarnier, L. P.; Casemiro, N. S.; Silva, D. B.; Cavalcanti, T. B.; Raman, V.; Khan, I. A.; Gasparotto Junior, A.; Budel, J. M. (2020). *Cuphea calophylla* var. *mesostemon* (Koehne) S.A. Graham: A Whole-Ethnopharmacological Investigation. *J Med Food* 24 (4), 394-410.
- Konyar, S. T.; Dane, Öztürk, N.; Dane, F. (2014). Occurrence, types and distribution of calcium oxalate crystals in leaves and stems of some species of poisonous plants. *Bot Stud* 55 (32), 1-9.
- Lersten, N.R.; Horner, H.T. (2011). Unique calcium oxalate “duplex” and “concretion” idioblasts in leaves of tribe Naucleaeae (Rubiaceae). *Am J Bot* 98 ,1-11.
- Meric, C. (2009). Calcium oxalate crystals in some species of the tribe Inuleae (Asteraceae). *Acta Biol Crac Ser Bot* 51 , 105-110.
- Oliveira, A. M. A.; Santos, V. L. P.; Franco, C. R. C.; Farago, P. V.; Duarte, M. R.; Budel, J. M. (2011). Comparative morpho-anatomical study of *Baccharis curitybensis* Heering ex Malme and *Baccharis spicata* (Lam.) Baill. *Lat Am J Pharm* 30 (8), 1560-1566.
- Pauser, M. S.; Borsato, T. O.; Almeida, V. P.; Raman, V.; Justus, B.; Pereira, C. B.; Flores, T. B.; Maia, B. H. N. S.; Meneguetti, E.; Kanunfre, C. C.; Paula, J. F. P.; Farago, P. V.; Budel, J. M. (2021). *Eucalyptus cinerea* : Microscopic profile, chemical composition of essential oil and its antioxidant, microbiological and cytotoxic activities. *Braz Arc Biol Technol* 64 , 1-19.
- Pritchard, S.G.; Prior, S.A.; Rogers, H.H.; Peterson, C.M. (2000). Calcium sulfate deposits associated with needle substomatal cavities of container-grown longleaf pine (*Pinus palustris*) seedlings. *Int J Plant Sci* 161 , 917-923.
- Raman, V.; Horner, H. T.; Khan, I. A. (2014). New and unusual forms of calcium oxalate raphide crystals in the plant kingdom. *J Plant Res*127 (6), 721-730.
- Santos, S. R.; Marchiori, J. N. C.; Siegloch, A. M.; Oliveira-Deble, A. S. (2012). Anatomia da madeira de duas espécies de *Baccharis* nativas do Rio Grande do Sul. *Balduinia* 36 , 03-11.
- Santos, V. L. P.; Franco, C. R. C.; Amano, E.; Messias-Reason, I. J.; Budel, J. M. (2015). Anatomical investigations of *Piper amalago*(jaborandi-manso) for the quality control. *Rev Bras Farmacogn* 25 , 85-91.
- Santos, V. L. P.; Raman, V.; Bobek, V. B.; Migacz, I. P.; Franco, C. R. C.; Khan, I. A.; Budel, J. M. (2018). Anatomy and microscopy of *Piper caldense* , a folk medicinal plant from Brazil. *Rev Bras Farmacogn* 28 , 9-15.
- Saulle, C. C.; Raman, V.; Oliveira, A. V. G.; Maia, B. H. L. N. S.; Meneghetti, E. K.; Flores, T. B.; Farago, P. V.; Khan, I. A.; Budel, J. M. (2018) Anatomy and volatile oil chemistry of *Eucalyptus saligna* cultivated in South Brazil. *Rev Bras Farmacogn* 28 , 125-134.
- Silva, R.J.F.; de Aguiar-Dias, A.C.A.; de Mendonça, M.S. (2014). Rosetas e con-crescências cristalinas silicificadas em *Piper*(Piperaceae): registros inéditos de macropadrões. *Acta Amazon* 44 , 435-446.
- Smith, J. A. (2012). *Geometric, Algebraic and Topological Connections in the Historical Sphere of the Platonic Solids* . University of Nevada, Reno.

Souza, J. P.; Santos, V. L. P.; Franco, C. R. C.; Bortolozo, E. A. F. Q.; Farago, P. V.; Matzenbacher, N. I.; Budel, J. M. (2011). *Baccharis rufescens* Spreng. var. *tenuifolia* (DC.) Baker: contribuição ao estudo farmacognóstico. *Rev Bras Pl Med* 15 (4), 566-574.

Storey, R.; Thomson, W. W. (1994). An X-ray microanalysis study of the salt glands and intracellular calcium crystals of *Tamarix* . *Ann Bot* 73 , 307-313.

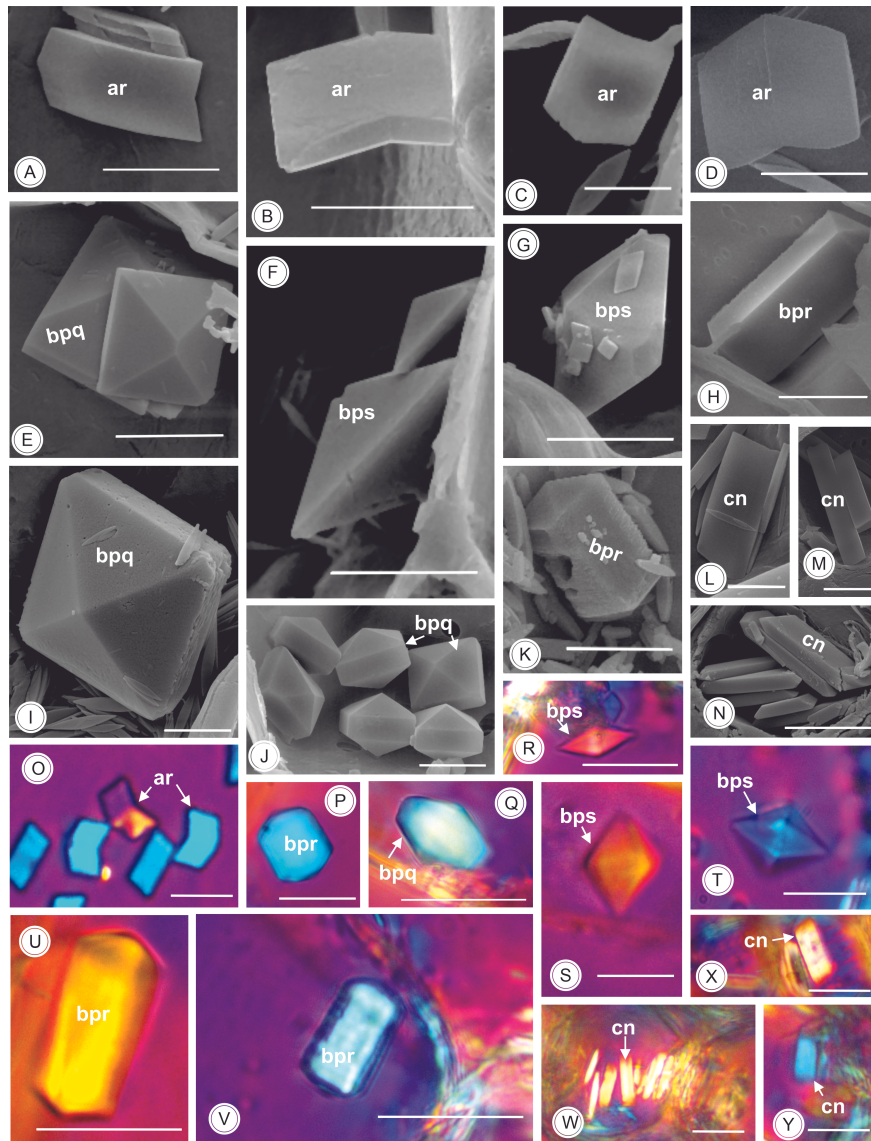
Sun, X. Y.; Ouyang, J. M.; Zhu, W. Y; Li, Y. B.; Gan, Q. Z. (2015). Size-dependent toxicity and interactions of calcium oxalate dehydrate crystals on Vero renal epithelial cells. *J Mater Chem B* 3 ,1864-1878.

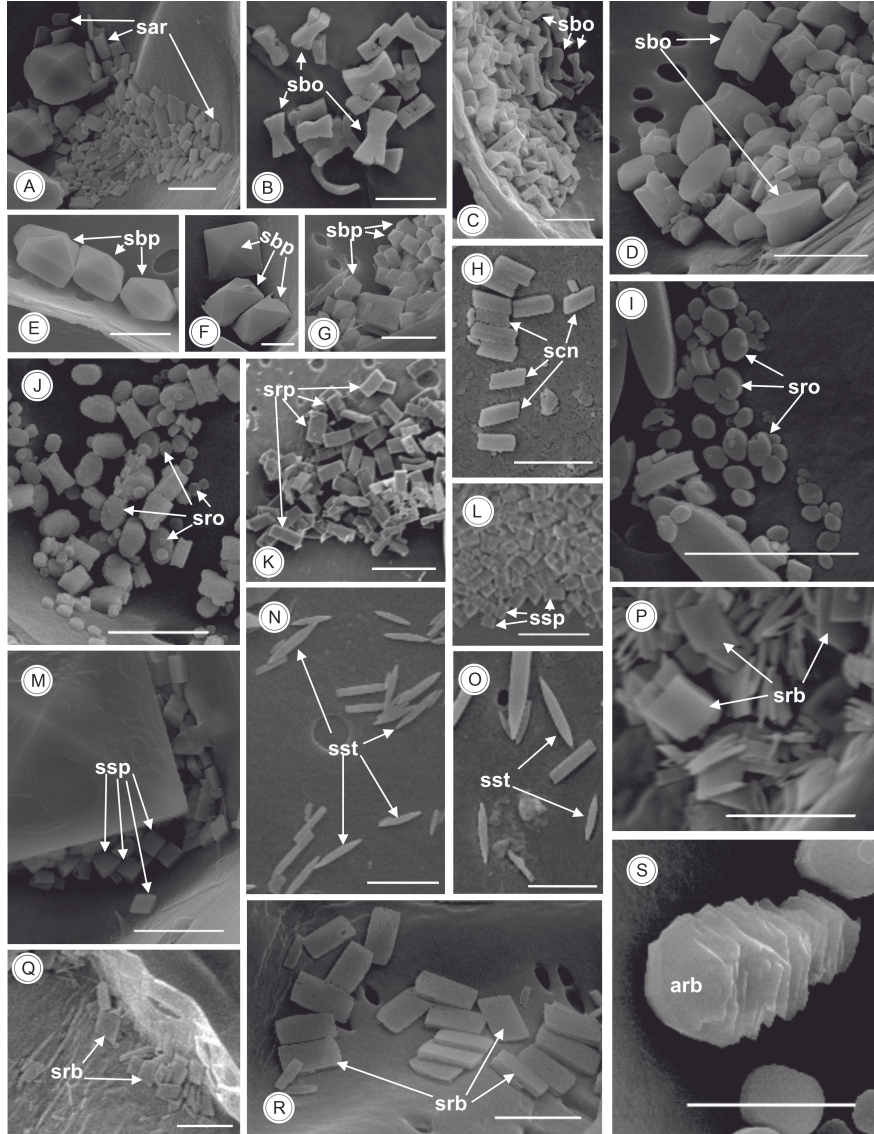
Uloth, M. B.; Clode, P. L.; You, M. P.; Barbetti, M. J. (2015). Calcium oxalate crystals: An integral component of the *Sclerotinia sclerotiorum* / *Brassica carinata* Pathosystem. *Plos One*10 (3), 1-15.

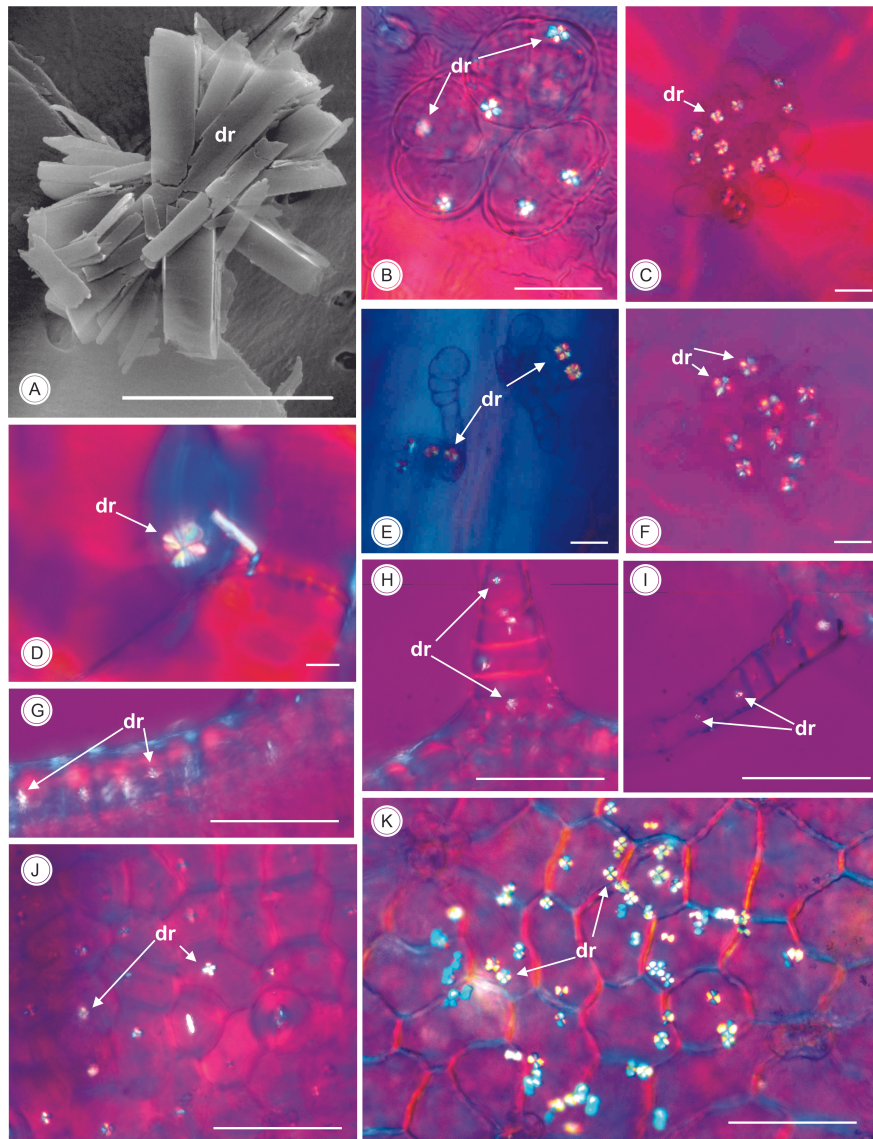
Upton, R.; Graff, A.; Jolliffe, G.; Länger, R.; Williamson, E. (2011). American herbal pharmacopeia botanical pharmacognosy: Microscopic characterization of botanical medicines, pp.30-46. CRC Press.

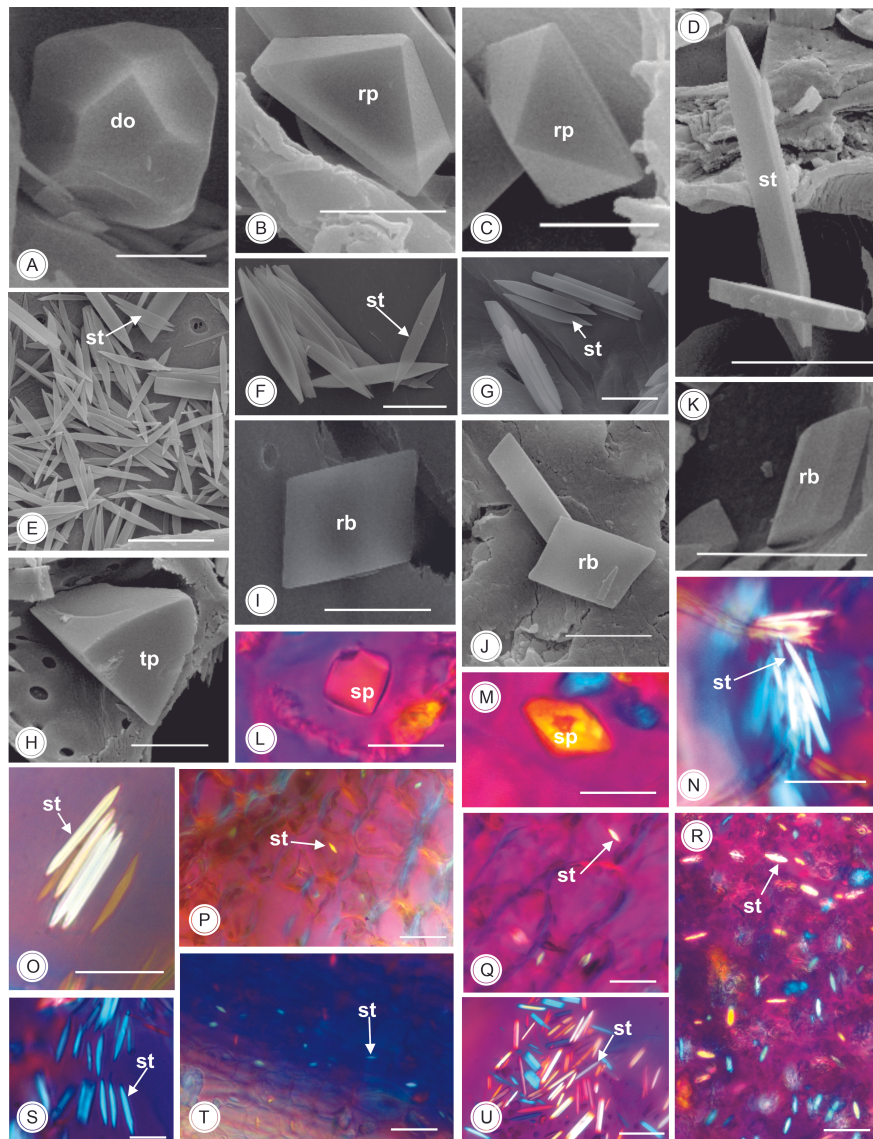
Webb, M. A. (1999). Cell-mediated crystallization of calcium oxalate in plants. *The Plant Cell* 11 , 751-761.

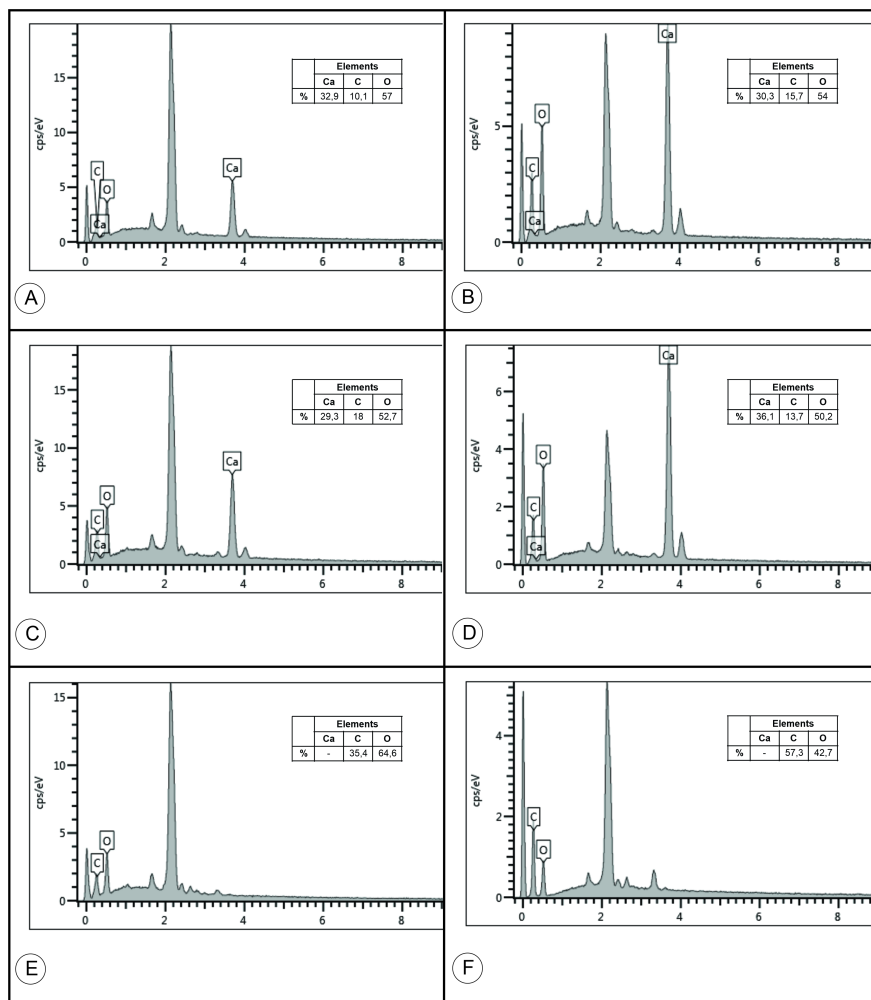
Weiner, S.; Dove, P. (2003). An overview of biomineralization processes and the problem of the vital effect. *Rev Mineral Geochem* 54 , 1-29.

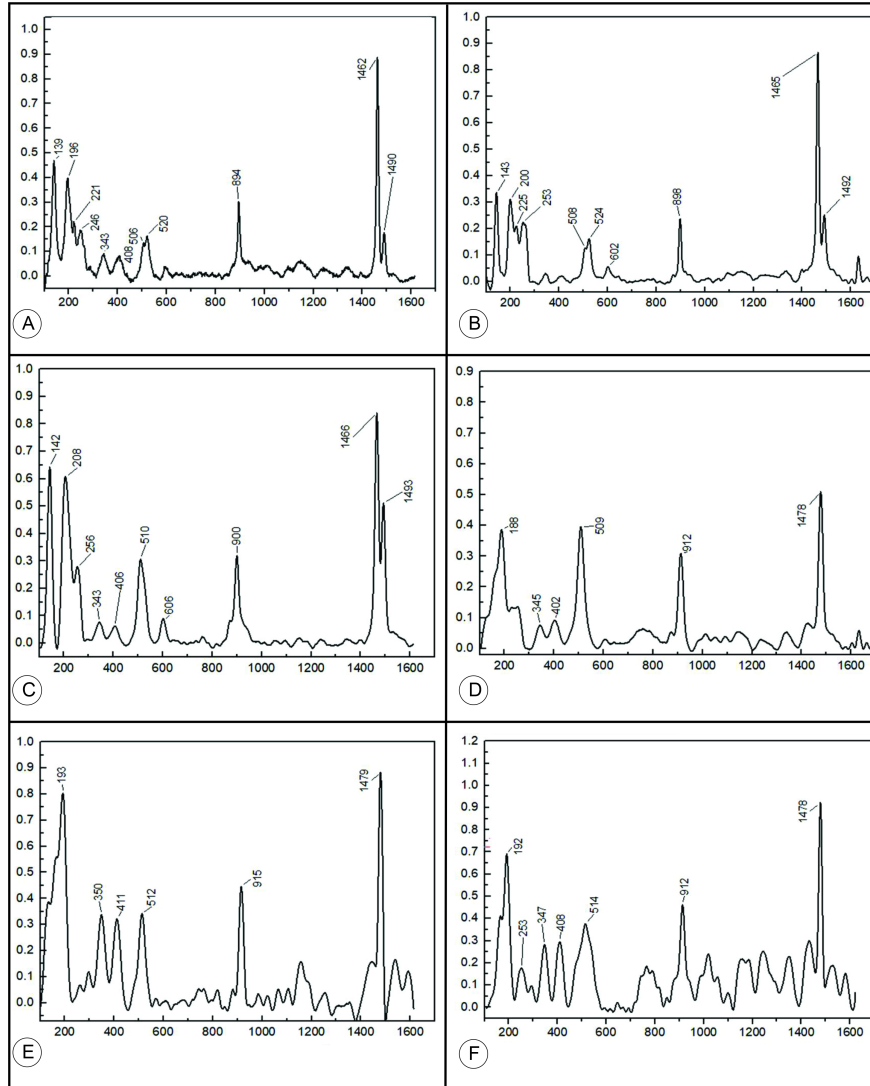












Hosted file

Table 1. Baccharis (Asteraceae) sampling species list subgenus and section placement collection location available at <https://authorea.com/users/580531/articles/621581-calcium-oxalate-crystal-macropattern-and-its-usefulness-in-the-taxonomy-of-baccharis-asteraceae>

Hosted file

Table 2 Morphotype and localization of crystals in the 44 investigated Baccharis (Asteraceae) species.d available at <https://authorea.com/users/580531/articles/621581-calcium-oxalate-crystal-macropattern-and-its-usefulness-in-the-taxonomy-of-baccharis-asteraceae>